参赛学生姓名: 廖毅夫

中学: 武汉爱莎文华学校

省份: 湖北

国家/地区:中国

指导老师姓名: 阮锦龙张帆

指导老师单位:武汉爱莎文华学校

论文题目: C-TranAD: A Complex-Valued Transformer-

based Anomaly Detection Model for Multivariable

Sequences and Its Application in Eddy Current Testing

C-TranAD: 一种复数域扩展的多变量序列异常检测模型及其在涡流缺陷检测中的应用

廖毅夫 武汉爱莎文华高级中学 Finder.liao26@isawuhan.com

摘要

涡流检测是较为常用的工业结构健康检测方法,传统上依赖人工分析检测信号以判定缺陷位置与类型。然而,该方法不仅过程复杂、准确率有限,而且结果高度依赖专家经验。近年来,深度学习方法被引入涡流信号分析,显著提升了检测的自动化水平。但涡流信号本质上为复数形式,包含幅值与相位双重信息,而现有大多数深度学习模型仍基于实数域建模,仅利用幅值或经手工提取的特征,难以充分利用多频率涡流信号中的信息。针对上述问题,本文提出了一种新型复数域时序异常检测网络—C-TranAD(Complex-valued Transformer-based Anomaly Detection)。该方法全面扩展至复数域,能够端到端地处理多频率涡流信号,避免了特征丢失与信息冗余,其主要创新包括:

- 1. 构建高质量涡流缺陷检测数据集:构建专有涡流缺陷检测数据集 SGT-ECT-13C5F,保留复数幅相特征并涵盖典型缺陷模式,为模型训练与评估提供可靠基准。
- 2. 复数域端到端建模: 首次将 TranAD 系统性扩展至复数域,实现对涡流信号的端到端 表征,完整保留幅值—相位耦合特征,并在多频率场景下提升缺陷模式刻画能力。
- 3. 可学习复数激活函数与分层分类机制:提出可学习的复数激活函数与分层分类机制,通过自适应非线性调节与多分支层次化表征,既保证了度量方式符合涡流物理机理并具备鲁棒性,又显著提升了模型对细微相位扰动与复杂缺陷模式的敏感性。

本文在自建多频率涡流缺陷数据集上进行了系统实验,结果表明 C-TranAD 准确率高达 96%,在检测准确率、召回率及鲁棒性方面均显著优于实数域 TranAD 及其他主流方法。该研究为复数域深度学习在涡流检测中的应用提供了新的思路,并为多频率信号下的缺陷识别奠定了方法学基础。

关键词: TranAD, 复数神经网络, 涡流缺陷检测, 复数域激活函数

C-TranAD: A Complex-Valued Transformer-based Anomaly Detection Model for Multivariable Sequences and Its Application in Eddy Current Testing

Yifu Liao ISA Wenhua Wuhan High School Finder.liao26@isawuhan.com

Abstract

Eddy current testing (ECT) is a widely used method for industrial structural health monitoring. Traditionally, it relies on manual interpretation of detection signals to identify the location and type of defects. However, this process is complex, has limited accuracy, and heavily depends on expert experience. In recent years, deep learning has been applied to ECT signal analysis, greatly improving the level of automation. Nevertheless, ECT signals are inherently complex-valued, containing both amplitude and phase information. Most existing deep learning models are real-valued, exploiting only amplitudes or hand-crafted features, which limits their ability to fully utilize the rich information in multi-frequency ECT signals.

To address this challenge, we propose C-TranAD (Complex-valued Transformer-based Anomaly Detection), a novel time-series anomaly detection network in the complex domain. C-TranAD enables end-to-end processing of multi-frequency ECT signals, avoiding feature loss and information redundancy. Its main contributions are as follows:

- 1. High-quality ECT defect dataset: We construct a proprietary dataset, SGT-ECT-13C5F, that preserves complex amplitude–phase features and covers typical defect patterns, providing a reliable benchmark for model training and evaluation.
- 2. End-to-end complex-domain modeling: We extend TranAD into the complex domain for the first time, achieving end-to-end representation of ECT signals. This design fully preserves coupled amplitude—phase features and improves the characterization of defect patterns in multi-frequency scenarios.
- 3. Learnable complex activation and hierarchical classification: We introduce learnable complex activation functions and a hierarchical classification mechanism. Through adaptive nonlinearity and multi-branch hierarchical representations, this approach ensures physical consistency with ECT principles, enhances robustness, and improves sensitivity to subtle phase variations and complex defect patterns.

Extensive experiments on our multi-frequency ECT dataset demonstrate that C-TranAD achieves an accuracy of up to 96%, significantly outperforming real-valued TranAD and other mainstream methods in terms of detection accuracy, recall, and robustness. This work provides new insights into the application of complex-valued deep learning to ECT and establishes a methodological foundation for defect identification in multi-frequency settings.

Keywords: TranAD, Complex-valued Neural Network, Eddy Current Testing, complex domain activation function

Table of Contents

摘要	1
Abstract	2
1. Introduction	4
2 Related Work	7
2.1 Eddy Current Signal Analysis	7
	8
	9
2.4 Summary	
3. Methodology	
3.1 Dataset and Preprocessing	
3.2 C-TranAD	11
3.2.1 C-TranAD overall model architecture	
3.2.2 Learnable multiple activation functions	12
3.2.3 Multi-scale complex classification head	15
3.2.4 Design of complex domain anomaly metrics	17
3.3 Training Strategies	
4. Experimental results and comparison	19
4.1 Experimental setup	19
4.2 Experimental Result Analysis	20
4.2.1 Comparative Analysis	20
4.2.2 Ablation Study Analysis	23
5. Analysis and Discussion	25
6. Conclusion	27
Reference	28
致谢	31

1. Introduction

Nuclear energy serves as a highly efficient and clean energy source, holding a significant position in the global energy structure [1]. As shown in Figure 1, the heat transfer tube bundle within a steam generator acts as a critical barrier between the primary and secondary circuits of a reactor. Its structural integrity is directly related to the containment of radioactive materials, the operational safety of the power plant, and the efficiency of energy conversion [2]. However, under long-term exposure to complex conditions such as high temperature, high pressure, fluid erosion, and corrosion, the heat transfer tubes are highly susceptible to defects like cracks and thinning [3]. Once a defect destabilizes and propagates, it can lead to severe radioactive leakage incidents with catastrophic consequences. Therefore, conducting regular, efficient, and precise in-service inspections to promptly identify and evaluate heat transfer tube defects is an essential measure to ensure the safe and reliable operation of nuclear power plants [4].

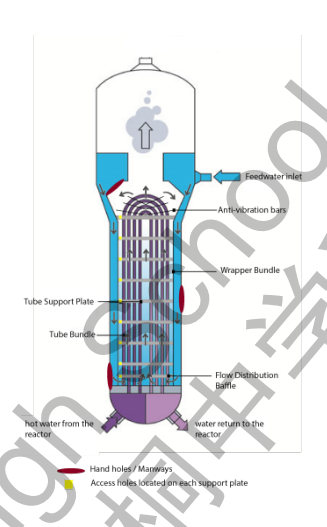


Figure 1. Typical heat exchanger: nuclear power plant steam generator

In this process, complex signal processing plays a crucial role. As a key direction in modern signal and information processing, complex-domain methods are widely applied in fields such as communications, energy, medical imaging, and structural health monitoring. Their core value lies in the ability to simultaneously represent both amplitude and phase, thereby more completely characterizing the dynamic properties of a physical system. For the eddy current inspection of steam generator heat transfer tubes, the impedance signal naturally exists in a complex form, where the coupled changes in amplitude and phase directly reflect the material's internal structural state and potential defects. Among the various non-destructive testing (NDT) techniques, Eddy Current Testing (ECT) has become the preferred method for in-service inspection of steam generators and various heat exchangers due to its high sensitivity, high detection speed, and non-contact nature [5, 6]. This technique works by inducing an eddy current in a conductive tube using a probe coil and then identifying defects by measuring changes in the complex impedance of the probe coil caused by these defects. The resulting complex signal contains rich amplitude and phase information, which is a critical basis for assessing the integrity of the tube wall [7,8,9]. Therefore, eddy current testing has become the most practical and scientifically significant inspection method for steam generator tubes in nuclear power plants, and improvements in its signal analysis and processing methods are of great importance for enhancing defect identification accuracy and

ensuring the operational safety of nuclear power plants [10]. However, due to the diversity of nuclear power plant types in China, different heat exchangers exhibit significant variations in heat transfer tube materials, manufacturing processes, and structural features [11]. Coupled with complex operating conditions and high-risk inspection environments, the processing and analysis of eddy current signals face immense challenges.

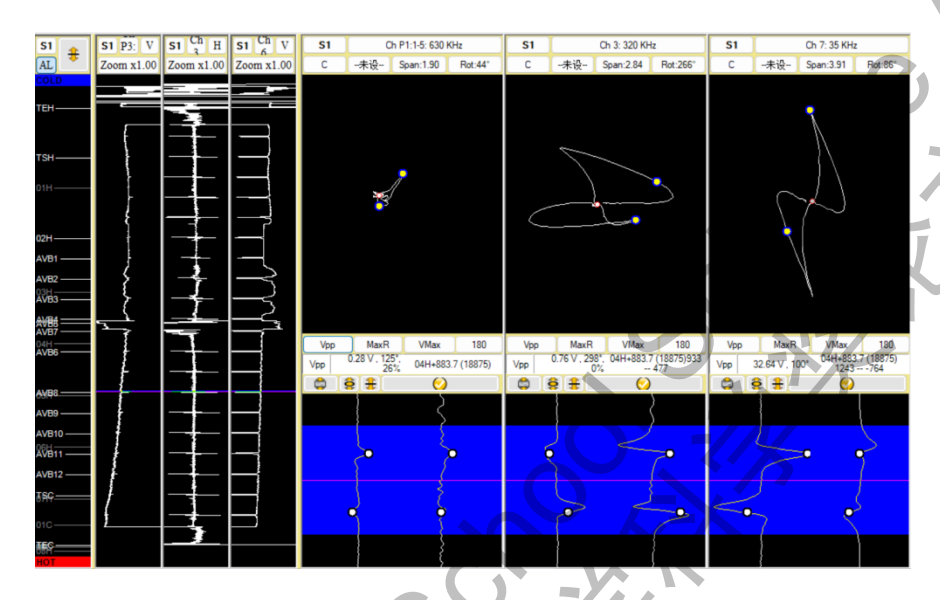


Figure 2. Typical multi-channel eddy current signal diagram of a heat exchanger heat transfer tube

As shown in Figure 2, detection signals are often accompanied by strong field noise [12] and are interfered with by structural factors such as tube sheets, support plates, tube expansions, and bends, which can mask defect signatures [13, 115]. The current signal interpretation still relies on experienced professionals [16], who must manually identify faint defect signals. This method is not only inefficient and costly but is also often influenced by subjective factors. Concurrently, with the advancement of signal acquisition technology, the rate of data acquisition has increased exponentially, but manual analysis can no longer match this in terms of speed and accuracy, failing to meet current inspection demands.

To resolve this contradiction, researchers have begun to explore the introduction of deep learning methods to achieve automated analysis of eddy current signals [17, 18]. In recent years, deep learning has offered new avenues for the intelligent analysis of eddy current signals. However, existing methods still face two main limitations. First, in terms of task modeling, most methods simplify eddy current inspection into a supervised classification problem, training models to identify "a specific type of defect" versus "no defect"[19]. This approach not only relies on a large amount of diverse labeled data but also has poor generalization capabilities for new or rare defects not seen during training[20]. Second, regarding signal representation, current methods commonly split the complex impedance signal into two independent real-valued channels—real and imaginary parts—for processing. This practice disrupts the intrinsic structure of the complex signal, particularly neglecting the phase angle feature. Phase information is crucial for distinguishing between defects and structural interferences like tube sheets and support plates; its loss severely compromises the model's detection accuracy.

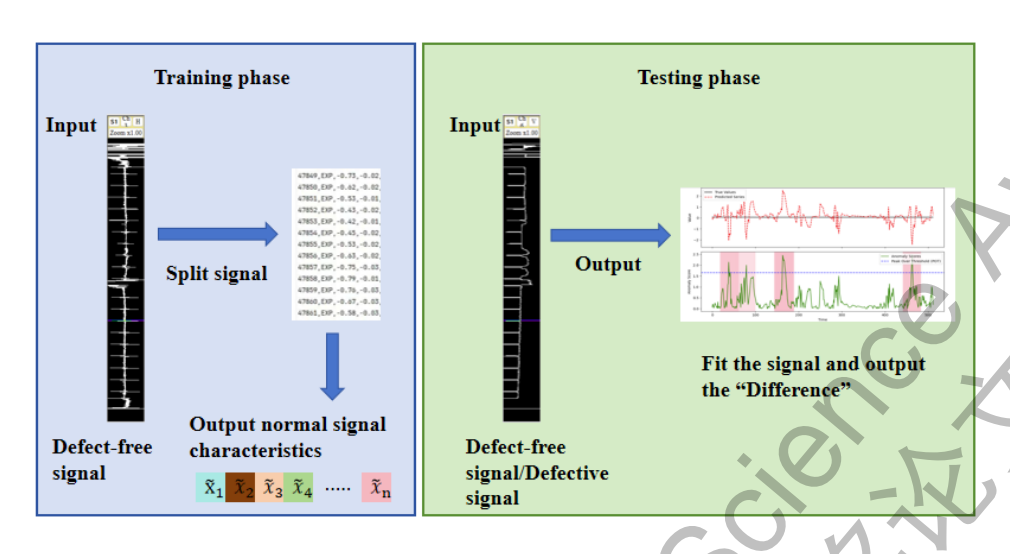


Figure 3 C-TranAD model structure

Based on the issues described, this paper introduces a completely new defect detection paradigm. Instead of directly modeling the task as a classification problem, we redefine it as a reconstructionbased anomaly detection problem. The core idea is to leverage the powerful sequence modeling and representation capabilities [21] of a model to learn only the intrinsic patterns of "defect-free" normal eddy current signals and use this knowledge to accurately reconstruct them. As illustrated in Figure 3, during the training phase, the model is exposed only to normal eddy current signals, gradually capturing their coupled amplitude and phase characteristics to form a generator that highly fits the normal patterns. During the detection phase, when a new eddy current signal is input, the model attempts to reconstruct it based on the learned normal patterns. If the input signal is indeed defect-free, the original and reconstructed signals will be highly similar, resulting in a minimal reconstruction error. If a defect is present, its amplitude and phase characteristics will deviate from the learned patterns, producing a significant reconstruction error. By setting an appropriate threshold, we can determine the presence of a defect based on the magnitude of this error. Building upon this foundation, the C-TranAD model proposed in this paper further achieves end-to-end modeling in the full complex domain, avoiding the structural information loss caused by splitting complex signals into real/imaginary channels in traditional methods. Specifically, we have incorporated learnable complex activation functions, a complex-domain anomaly measure, and a hierarchical classification mechanism into the architecture. This allows the model to simultaneously capture and amplify subtle fluctuations in both amplitude and phase during the reconstruction process. This design not only preserves the geometric integrity of the eddy current signal in the complex plane but also endows the model with stronger hierarchical discrimination and anomaly amplification capabilities, enabling it to exhibit higher sensitivity to small phase perturbations caused by defects. The method proposed in this paper has achieved excellent results in practical engineering applications. In real-world detection tasks, the model can reach an accuracy of 96%, significantly enhancing the reliability of defect identification. Furthermore, due to its end-to-end automated processing capability, its detection workflow is simple and efficient, making it directly applicable and scalable for industrial field use.

The main contributions of this paper are:

- 1) Dataset Construction and Validation: We constructed a proprietary eddy current defect detection dataset, my_data, which preserves complex amplitude-phase information while covering typical defect patterns. This dataset provides a reliable benchmark for model training and evaluation. Experiments have validated that C-TranAD is significantly superior to real-valued methods and other mainstream models in terms of accuracy, robustness, and false alarm rate control.
- 2) End-to-End Modeling in the Complex Domain: We achieved a systematic extension of the TranAD model to the complex domain for the first time, proposing the C-TranAD model. By preserving and utilizing the amplitude-phase coupling relationship end-to-end, the model can more accurately identify defects under multi-frequency conditions, avoiding the information loss and feature fragmentation inherent in real-valued methods. This significantly enhances the modeling and detection capabilities for complex eddy current signals.
- 3) Learnable Complex Activation Functions and Hierarchical Classification Mechanism: We proposed an improved Cardioid activation function, introducing learnable frequency and phase offset parameters to its phase-sensitive base. This allows the network to adaptively adjust its non-linear response and output range, enhancing its sensitivity to subtle phase perturbations and complex defect patterns. Additionally, we designed a hierarchical complex classification head that fuses the results from different activation function branches, achieving a hierarchical representation and defect discrimination across multiple frequency channels. This mechanism not only aligns with the physical principles of eddy current inspection and offers robustness but also further improves the model's discriminative ability in complex operating conditions.
- 4) Complex-Domain Anomaly Measure Design: We introduced an amplitude-phase joint complex distance metric, extending the reconstruction error from a real-valued norm to a complex-domain consistency measure. This design considers both amplitude deviation and phase drift, is robust to rotation and scaling, better conforms to the physical characteristics of eddy current signals, and significantly enhances detection stability.

2 Related Work

2.1 Eddy Current Signal Analysis

Eddy current testing (ECT) is an important non-destructive testing technique. Its signals naturally take a complex-valued form (amplitude and phase). In ECT signal analysis, traditional methods largely rely on manual feature extraction and interpretation of complex impedance signals. Early studies typically extracted geometric features from the impedance plane (Impedance Plane Plot, i.e., amplitude—phase Lissajous patterns) [22], such as loop size and angle, and used them as inputs to classifiers. These approaches depend heavily on manually designed features, suffer from limited information utilization, and struggle to adapt to complex operating conditions.

With the development of machine learning and deep learning, researchers have gradually attempted to transform eddy current signals into alternative representations [17] and then apply intelligent algorithms for defect identification. For example, some works convert time-domain or frequency-domain signals into time-frequency images, which are then fed into convolutional

neural networks (CNNs) or attention-based models for classification [23, 24]. Miao et al. transformed eddy current weld defect signals into time—frequency images and input them to a VGG network to achieve defect type recognition [25]. Gao et al. compared ResNet, DenseNet, and spatiotemporal self-attention networks on eddy current image data, finding that incorporating attention mechanisms can significantly improve recognition accuracy [26].

Overall, deep learning methods have gradually been applied to ECT signal processing. However, most existing studies still rely on signal transformation and feature engineering, i.e., converting raw signals into images or hand-crafted features before modeling. This not only introduces additional preprocessing complexity but may also cause information loss and noise amplification, limiting the model's ability to exploit intrinsic signal characteristics. In contrast, end-to-end deep learning directly based on raw complex-valued eddy current signals remains relatively underexplored. Existing methods often represent complex impedance by separating the real and imaginary parts for independent modeling [27], which breaks the intrinsic coupling of the signals and fails to fully leverage phase information—a key characteristic.

2.2 Time-Series Anomaly Detection

ECT signals are inherently time-series data, making it possible to draw on advances in time-series anomaly detection. A large body of research has emerged in this domain. Traditional approaches include statistical thresholding, Isolation Forest, One-Class Support Vector Machines (One-Class SVM), and autoencoder (AE)—based methods relying on reconstruction errors [28-31]. These approaches have achieved certain success in anomaly detection for various sensor data, but they generally depend on manual features and perform poorly on high-dimensional multivariate time-series data.

In recent years, the rapid progress of deep learning has driven significant advances in time-series anomaly detection. Recurrent neural networks (RNNs) and their variants such as LSTMs have been widely used to model temporal dependencies [32]. Variational Autoencoders (VAEs) and Generative Adversarial Networks (GANs) have also been introduced into generative anomaly detection frameworks.

With the rise of Transformer architectures, their powerful attention mechanisms enable simultaneous modeling of both long- and short-term dependencies, offering new opportunities for anomaly detection [33]. Among these, TranAD is a representative method [21, 34]. It leverages multi-head attention to capture global patterns in time series and incorporates self-conditioning training and adversarial training to improve generalization. Furthermore, it employs model-agnostic meta-learning (MAML) to enhance adaptability in few-shot scenarios. Experimental results demonstrate that TranAD significantly outperforms state-of-the-art methods of its time on multiple public datasets [21, 34, 35], while also achieving substantial improvements in training efficiency. These findings highlight the great potential of Transformer-based deep models in time-series anomaly detection.

2.3 Complex-Valued Neural Networks

Since ECT signals are inherently complex-valued, complex-valued neural networks (CVNNs) have become a promising research direction. Research on CVNNs dates back several decades and has been explored in fields such as communication signal processing, radar imaging, and magnetic resonance imaging (MRI) [36, 37]. The core challenge lies in designing appropriate complex operations and activation functions that allow the network to effectively model amplitude–phase coupling in complex data.

Existing complex activation functions can be broadly divided into two categories: one separates the real and imaginary parts for independent operations [38] (e.g., applying sigmoid or tanh separately), while the other performs unified amplitude—phase mappings [39]. Among these, the Cardioid activation function has attracted wide attention due to its unique phase-sensitive properties [40]. It preserves the phase of the input while modulating the output amplitude: inputs with phases near the negative real axis are strongly suppressed, while those near the positive real axis are passed almost unchanged, thereby achieving a ReLU-like nonlinear selectivity. This property makes it particularly effective for modeling phase information in complex signals.

Nevertheless, most studies on CVNNs have focused on signal reconstruction and classification, while systematic exploration in time-series anomaly detection remains scarce. At the same time, multi-scale modeling has proven effective in computer vision and time-series analysis: multi-branch architectures can capture information at different spatial scales in vision tasks, while in time-series tasks, capturing features across different temporal windows or frequency bands is critical for identifying diverse anomaly patterns [41]. This provides new research directions for complex-domain time-series anomaly detection.

2.4 Summary

In summary, the complex nature of ECT signals makes joint modeling of amplitude and phase essential for defect identification. However, existing methods either rely on hand-crafted features and signal transformation, with limited information utilization, or employ deep learning in the real domain, which disrupts amplitude—phase coupling. Meanwhile, recent advances in time-series anomaly detection—particularly Transformer-based approaches—demonstrate strong modeling capabilities but have not been tailored to complex-valued signals. CVNNs show great potential for modeling complex data, yet the design of activation functions and multi-scale mechanisms for anomaly detection tasks remains underexplored. Therefore, there is an urgent need for an end-to-end time-series anomaly detection approach in the complex domain, one that fully exploits both amplitude and phase information while incorporating multi-scale and hierarchical mechanisms to meet the practical demands of industrial scenarios such as ECT.

3. Methodology

3.1 Dataset and Preprocessing

The dataset used in this study was sourced from eddy current inspections of steam generator heat transfer tubes conducted during a scheduled refueling outage at a nuclear power plant in China. This scenario has significant engineering relevance: various defects can occur during the service life of heat transfer tubes, with external wall wear (Wear, WER) being one of the most common and high-risk types. WER signals are often complex, potentially causing both amplitude spikes and phase shifts, thus imposing high demands on the robustness and sensitivity of anomaly detection algorithms.

The data was collected using the C-Eddy eddy current inspection system, which includes a heat transfer tube positioning robot, a probe pusher/puller, an eddy current instrument, and data acquisition software. The collection process is as follows: the eddy current instrument generates alternating currents at 5 different frequencies, which are time-division multiplexed and applied to the probe coil as it moves at a constant speed inside the tube. When the tube is intact, the probe's impedance remains stable. If a defect or structural change is present, the impedance will be perturbed. The eddy current instrument converts these impedance changes into digital signals via an analog-to-digital converter and transmits them to a host computer for storage via the TIP-IP protocol. Each heat transfer tube (approximately 20-25 meters long) corresponds to one data file, containing 5 detection frequencies and 10 independent channels, plus 3 software-generated differential channels, for a total of 13 channels. Each channel contains about 60,000 to 100,000 complex sample points (real and imaginary parts), recording the impedance changes throughout the inspection process.

To ensure the comparability of signals collected under different conditions, we developed a dedicated data conversion and preprocessing module to systematically standardize and calibrate the raw signals:

- 1) Signal Centering: The signal segment from a defect-free section is shifted to the virtual coordinate origin to eliminate DC offset caused by equipment configuration.
- 2) Phase Adjustment: As the phase angle is random across different acquisitions, a known defect (e.g., an artificial through-hole) is used for uniform calibration. For example, the differential channel is adjusted to 40° to ensure consistency between channels.
- 3) Amplitude Adjustment: The raw signal amplitude is a relative value, not a physical voltage. Therefore, a reference defect (e.g., a through-hole or support plate signal) is used for amplitude normalization, setting it to a standard value.

In the subsequent data preparation stage, we performed mean normalization on the real and imaginary parts of the complex signal separately to eliminate deviations caused by workpiece differences and probe conditions. A light band-pass filter was applied to remove low-frequency drift and high-frequency noise. Finally, a sliding time window was used to segment the long sequence into fixed-length segments to maintain temporal and complex feature consistency. The final SGT-ECT-13C5F dataset includes several hundred labeled actual defects (mainly WER) and a large number of normal samples. The training set consists of defect-free segments for learning

the normal pattern, while the test set contains various types of defective segments, covering everything from minor perturbations to significant defects. Although this dataset is not publicly available, it is highly representative and engineering-realistic, providing a solid foundation for the end-to-end learning and validation of the proposed C-TranAD model in the complex domain.

3.2 C-TranAD

3.2.1 C-TranAD overall model architecture

The C-TranAD model is based on the Transformer encoder-decoder framework of TranAD but has been systematically modified for complex data types and operators in its overall implementation. The model input is a complex time series of length T, $(Z_1,Z_2,Z_3...Z_T)$ where

$$Z_t = x_t + iy_t \quad (1)$$

In Equation 1, x_t and y_t represent the real and imaginary parts of the signal, respectively. The input can be equivalently represented as a two-channel real-valued sequence (real-imaginary), ensuring that the model can fully preserve the geometric integrity of the complex signal from the initial stage. Subsequently, the input signal undergoes feature modeling and reconstruction learning through several stacked complex Transformer encoder-decoder layers. Unlike traditional real-valued networks, every layer's parameters, weights, and operations in C-TranAD are implemented in the complex domain. This allows the model to directly capture the unique amplitude-phase coupling patterns of complex signals. Particularly in the design of the non-linear units, we introduced complex activation functions to ensure the effective preservation and modulation of phase information during forward propagation and feature transformation, significantly enhancing the model's sensitivity to subtle phase perturbations caused by defects.

In the output layer, C-TranAD employs a complex classification head to perform anomaly determination at each time point. Specifically, we designed a multi-scale parallel branch structure. The classification head consists of several parallel branches, each using a complex cosine activation function initialized with different parameters to selectively respond to different frequency components and phase shifts of the input features. This design allows the classifier to simultaneously focus on global trends and local perturbations at multiple scales, thereby more comprehensively distinguishing different types of defect patterns. The features extracted by each branch are further combined with a residual mechanism during the fusion stage and enhanced by amplitude-phase decomposition to increase feature diversity. Finally, an anomaly score or class label is output. The entire model is trained end-to-end. In an unsupervised setting, the complex reconstruction error serves as the training objective. To ensure the loss definition is consistent with the signal's physical mechanism, we introduced a complex-domain anomaly measure in the model, extending the traditional real-valued norm to a complex geometric distance that simultaneously considers amplitude and phase differences, thereby guiding parameter updates more accurately during backpropagation.

In summary, the C-TranAD method consists of three core components: (1) Complex Transformer Sequence Modeler: Learns the temporal dependencies of eddy current

signals complex feature representations of and the normal (2) Complex Multi-Scale Classification Head: Fuses feature representations at different frequencies and phase offsets to output anomaly score an or (3) Complex Anomaly Measure: A complex geometric distance defined by the joint error of amplitude and phase, used to guide reconstruction and classification optimization.

Through this design, C-TranAD integrates the strengths of reconstruction-based anomaly detection and discriminative classification. It possesses the ability to learn normal patterns in an unsupervised manner to discover anomalies, while also using a multi-scale discriminative mechanism to achieve direct classification of defects.

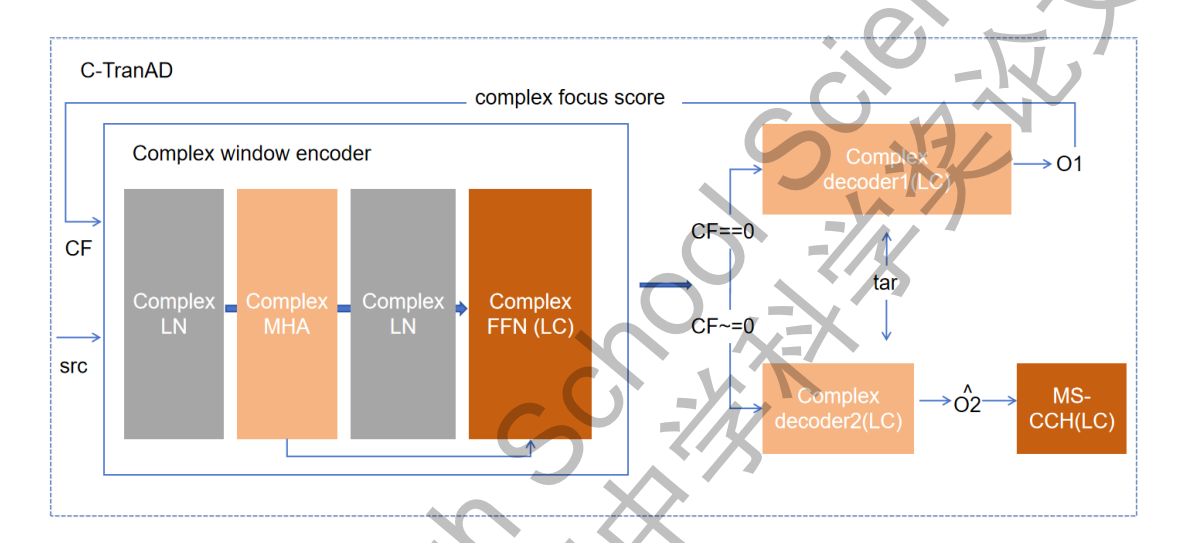


Figure 4. C-TranAD: Complex window encoder (Complex LN → Complex MHA → Complex LN → Complex FFN (LC)) → dual decoders: Decoder1(LC) → O1; Decoder2(LC)+CF → Ō2; MS-CCH (LC) produces anomaly score. Abbr.: LC=learnable Cardioid activation; CF=complex focus score; MS-CCH=Multi-Scale Complex(-Valued) Classification Head

3.2.2 Learnable multiple activation functions

In a complex neural network, the activation function not only performs non-linear transformation but also determines whether the model can effectively utilize the coupled amplitude and phase characteristics of complex signals. For eddy current inspection tasks, defects often manifest as phase shifts or flips. If the model relies solely on real-valued functions (like ReLU, Tanh), phase information will be weakened or even lost during propagation, making it difficult to capture significant defect features. Therefore, we chose to start with the Cardioid activation function and extend and improve it.

The Cardioid activation function was originally proposed with the goal of directly utilizing the phase information of the input in non-linear mapping. Its definition is:

$$f_{cardioid}(z) = \frac{1+\cos\theta}{2} \cdot z$$
 (2)

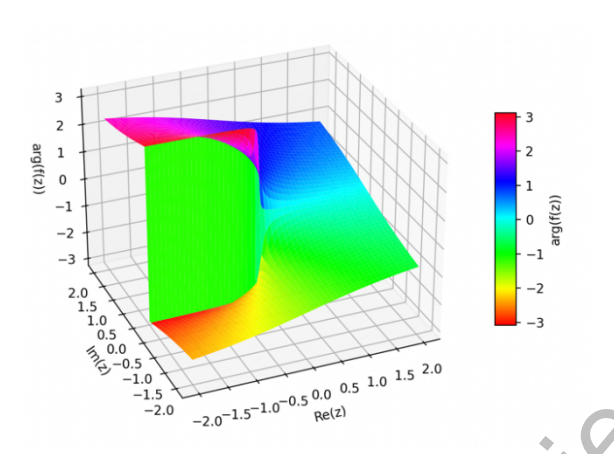


Figure 5. Graph of the Cardioid activation function

As shown in Function 2, the output preserves the input phase θ while its magnitude is scaled by a factor. Its effect is similar to the non-negative clipping of ReLU in the real domain. Cardioid allows the network to automatically emphasize components in the direction of the positive real axis (near phase 0) while suppressing components with phase deviation. This mechanism is particularly well-suited to the physical properties of eddy current signals: defects often cause phase shifts in the signal, and the Cardioid activation can naturally respond to these phase shifts, thereby enhancing the network's sensitivity to defect features. Although the Cardioid activation function emphasizes the importance of phase, its functional shape is fixed, leading to the following shortcomings:

- 1) Monotonic Phase Response: It always centers on the positive real axis, making it unable to adapt to tasks that require focusing on other phase regions.
- 2) Lack of Flexibility: It applies the same phase sensitivity pattern to all neurons, limiting the model's expressive power.
- 3) Poor Adaptability to Complex Defect Patterns: In actual eddy current signals, anomalies can manifest as large phase jumps, magnitude reductions, or composite perturbations. A fixed Cardioid function struggles to handle all these cases simultaneously. Therefore, directly using the original Cardioid is insufficient for high-precision anomaly detection.

To enhance flexibility, we propose an improved complex cosine activation function. Based on Cardioid, we introduce a learnable frequency factor ω and a phase offset φ . f_s denotes the Swish function, and β is a trainable parameter, allowing the $f_{\text{Learnable cardioid}}$ to have adaptive non-linear strength adjustment:

$$f_{Learnable\ cardioid}(z) = \frac{1 + \cos (\omega \theta + \phi)}{2} \cdot z \quad (3)$$
$$f_{S}(x) = \frac{x}{1 + e^{-\beta x}}$$

Here, ω determines the function's sensitivity to phase changes. When $\omega > 1$, the function oscillates more frequently within $[0,\frac{\pi}{2}]$, making it more sensitive to subtle phase perturbations. When $0 < \omega < 1$, the curve is smoother, suitable for modeling overall trends. φ shifts the function along the phase axis, allowing different neurons to focus on different phase regions, thus creating differentiated response patterns. After forward propagation, the total classification error E is given by the difference between the network output and the labels. Assuming the partial derivative of the classification error E with respect to the output a of $f_{\text{Learnable cardioid}}$ is

$$\frac{\partial E}{\partial a} = \frac{\partial E}{\partial \Re(a)} + j \frac{\partial E}{\partial \Im(a)}$$

Then, according to the complex chain rule and Equation (2), the partial derivative of E with respect to the input z of $f_{Learnable\ cardioid}$ is:

$$\frac{\partial E}{\partial \mathbf{Z}} = \frac{\partial E}{\partial \mathbf{R}(z)} + j \frac{\partial E}{\partial \mathfrak{F}(z)}$$

$$\frac{\partial E}{\partial \mathbf{R}(z)} = \frac{\partial E}{\partial \mathbf{R}(a)} \frac{\partial \mathbf{R}(a)}{\partial \mathbf{R}(z)} + \frac{\partial E}{\partial \mathfrak{F}(a)} \frac{\partial \mathbf{S}(a)}{\partial \mathbf{R}(z)}$$

$$\frac{\partial E}{\partial \mathbf{R}(a)} \frac{\partial \mathbf{R}(a)}{\partial \mathbf{R}(z)} = \frac{\partial E}{\partial \mathbf{R}(a)} (\frac{1}{2} f_s'(\mathbf{R}(z)) + \frac{1}{2} f_s'(\mathbf{R}(z)) \cos\theta + \frac{1}{2} f_s(\mathbf{R}(z)) \sin\theta \frac{\mathfrak{F}(z)}{|z|^2})$$

$$\frac{\partial E}{\partial \mathfrak{F}(a)} \frac{\partial \mathfrak{F}(a)}{\partial \mathfrak{R}(z)} = \frac{\partial E}{\partial \mathfrak{F}(a)} \frac{\partial \mathfrak{F}(a)}{\partial \mathfrak{F}(z)} + \frac{\partial E}{\partial \mathfrak{F}(a)} \frac{\partial \mathfrak{F}(a)}{\partial \mathfrak{F}(z)}$$

$$\frac{\partial E}{\partial \mathfrak{F}(a)} \frac{\partial \mathfrak{R}(a)}{\partial \mathfrak{F}(z)} = \frac{\partial E}{\partial \mathfrak{R}(a)} (-\frac{1}{2} f_s(\mathbf{R}(z)) \sin\theta \frac{\mathfrak{R}(z)}{|z|^2})$$

$$\frac{\partial E}{\partial \mathfrak{F}(a)} \frac{\partial \mathfrak{F}(a)}{\partial \mathfrak{F}(z)} = \frac{\partial E}{\partial \mathfrak{F}(a)} (\frac{1}{2} f_s'(\mathfrak{F}(z)) \cos\theta - \frac{1}{2} f_s(\mathfrak{F}(z)) \sin\theta \frac{\mathfrak{R}(z)}{|z|^2})$$

Where |z| represents the amplitude of the input complex number and f_s' is the derivative of f_s .

$$f_s'(x) = \frac{1}{1 + e^{-\beta x}} + \frac{x\beta}{1 + e^{-\beta x}} (1 - \frac{1}{1 + e^{-\beta x}})$$

It can be observed that the composite structure of $f_{Learnable\ cardioid}$ is fully differentiable, and this differentiability ensures seamless integration into the standard backpropagation framework. The steepness of the Swish activation curve is controlled by the learnable real-valued parameter β , and its gradient is expressed as:

$$\frac{\partial E}{\partial \beta} = \frac{\partial E}{\partial \Re(a)} \frac{\partial \Re(a)}{\partial \beta} + \frac{\partial E}{\partial \Im(a)} \frac{\partial \Im(a)}{\partial \beta}$$

$$\frac{\partial E}{\partial \Re(a)} \frac{\partial \Re(a)}{\partial \beta} = \frac{\partial E}{\partial \Re(a)} f_s(\Re(a)) \Re(a) (1 - \frac{1}{1 + e^{-\beta \Re(a)}})$$

$$\frac{\partial E}{\partial \Im(a)} \frac{\partial \Im(a)}{\partial \beta} = \frac{\partial E}{\partial \Im(a)} f_s(\Im(a)) \Im(a) (1 - \frac{1}{1 + e^{-\beta \Im(a)}})$$

Based on the above equations, the systematic adjustment of the parameter β enables comprehensive optimization of the activation module, thereby enhancing its performance. By making ω and φ learnable parameters, they are updated along with the network's weights and biases during training. This allows the network to form a rich combination of non-linear responses in the complex plane, achieving a transition from "fixed phase sensitivity" to "adaptive phase selectivity." It is important to note that after introducing learnable parameters, the activation function is no longer Holomorphic. However, we train the network by separately calculating the derivatives with respect to the real and imaginary parts, which has proven to be stable in practice. Similar approaches have been explored in previous research [42], but with the limited effect of simple biases. In contrast, our ω and φ provide a larger adjustment space, enabling the activation function to model complex features in a more flexible manner. This improvement is crucial for enhancing C-TranAD's ability to fit complex patterns.

3.2.3 Multi-scale complex classification head

In anomaly detection tasks, different types of anomalies often exhibit significant differences in time scales and signal patterns. Some anomalies are short-lived and bursty, appearing as high-frequency, small-scale features (e.g., transient pulses or spikes). Others are cumulative and slow-developing, appearing as low-frequency, large-scale changes (e.g., gradual signal drift). Furthermore, in the context of complex signals, an anomaly can manifest as a fluctuation in amplitude, a shift in phase, or both simultaneously. A single-structured output layer often struggles to concurrently address anomalies of different scales and feature dimensions.

To tackle this problem, this paper proposes a multi-scale complex classification head, MS-CCH (Multi-Scale Complex Classification Head). This module employs a multi-branch parallel architecture, where different branches use parameterized complex activation functions to achieve differential responses in the phase-amplitude space. This allows them to focus separately on high-frequency transient anomalies, low-frequency gradual anomalies, or amplitude/phase-dominant anomaly features. Ultimately, the outputs of the various branches are complementarily enhanced during a fusion stage to achieve unified discrimination of multiple anomaly types. This design equips the model with multi-scale and multi-modal discriminative capabilities, significantly improving its robustness and sensitivity in detecting complex anomaly patterns.

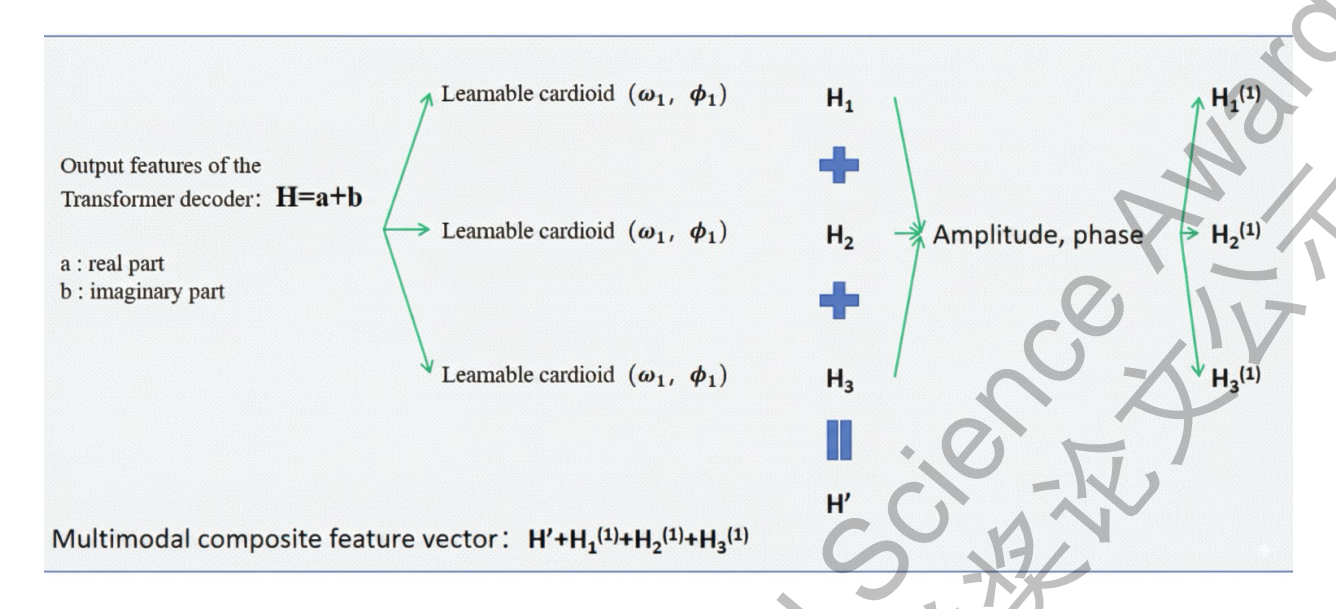


Figure 6. Classification head process

As shown in Figure 6, the classification head first receives the output feature H from the Transformer decoder and enhances its feature dimensionality through a complex linear projection layer to obtain a richer representation. Then, the features are fed in parallel into three branch subnetworks, each designed to model a different feature scale or frequency range. Specifically, each branch consists of a complex fully connected layer, a learnable complex activation function, and a complex batch normalization layer. It is important to emphasize that while the activation functions in the different branches have the same form, their parameters ω and φ are set differently. Although the activation form is the same, the differential settings of frequency scaling and phase offset create complementary selective responses to phase/frequency components. This is equivalent to implementing three distinct band-pass filters in the complex frequency domain (e.g., branch 1 focuses on low-frequency/global trends, branch 2 on mid-frequency structures, and branch 3 on high-frequency/transient perturbations or acts as a linear control to prevent overfitting). This mechanism allows each branch to be sensitive to different phase patterns and frequency components, thereby achieving an effect similar to multi-band filtering on the whole. Additionally, each branch incorporates a complex residual connection after activation, adding the input feature directly back to the output. This not only helps mitigate the vanishing gradient problem that can occur in deep complex networks and improves training stability but also establishes connections between features at different scales. This design ensures that if a certain type of anomaly is not prominent in one branch, it is likely to be captured in another, more suitable branch.

After processing through the three branches, we obtain three sets of feature representations at different scales, each containing real and imaginary parts. To get the final anomaly discrimination result, we employ a strategy that combines feature-level and decision-level fusion. For feature-level fusion, we concatenate the hidden feature vectors from the second-to-last layer (i.e., before the final classification layer) of each branch to form a comprehensive representation. To further enhance discriminative power, we explicitly add the magnitude and phase of the complex features during the concatenation process. For instance, for a complex feature, in addition to its real and imaginary parts, we append its magnitude and phase as additional dimensions. This preserves the

geometric structure of the complex numbers while providing the classifier with intuitive physical semantics. For decision-level fusion, we concatenate the real parts and imaginary parts of the three feature sets separately to obtain the fused complex feature H'. Then, a complex linear transformation and our Learnable Cardioid activation are applied to the concatenated result for non-linear refinement and normalization, achieving deep fusion of information across branches. This fused feature synthesizes discriminative information from different scales and frequencies, which can be viewed as a multi-perspective characterization of the original anomaly pattern. Finally, we concatenate the feature-level and decision-level fusion results again to form a multi-modal composite feature vector containing real, imaginary, amplitude, and phase components. This vector is fed into the final classifier to perform a binary classification, outputting the probability or label of a defect's presence.

The multi-scale complex classification head achieves comprehensive capture of complex anomaly patterns through its parallel branches and fusion mechanism. On the one hand, in the time dimension, branches with different depths or convolutional receptive fields can focus on shortterm bursty anomalies and long-term gradual anomalies, ensuring the model has multi-level sensitivity in the time domain. On the other hand, in terms of signal properties, the learnable complex activation functions with different parameter configurations allow each branch to form a differentiated response to magnitude perturbations or phase shifts, achieving fine-grained modeling of the multi-dimensional features of complex signals. Based on this, the fusion step integrates the features extracted by the different branches, ensuring that the final decision is based on multi-source information and avoiding the omission of any potential anomaly patterns. It is worth emphasizing that this structure, with a negligible increase in computational complexity, can respond to anomalies regardless of their manifestation (e.g., short pulses, slow drifts, magnitude spikes, or phase shifts) in the corresponding branches. Furthermore, the multi-branch structure enhances the system's redundancy and robustness: even if one branch fails or performs poorly in a specific scenario, the other branches can provide compensation, thereby improving the stability of the overall discrimination.

The proposed multi-scale complex classification head significantly enhances C-TranAD's ability to capture weak anomalies in complex backgrounds—both short-term and long-term anomalies are addressed in the time dimension, and both amplitude and phase anomalies are effectively characterized in the signal property dimension. From an innovation perspective, our fusion mechanism for hierarchical activation in the complex domain organically combines learnable activation functions with a multi-scale structure, opening up a new path for the hierarchical utilization of complex features. This provides universal reference value and promotional significance for deep anomaly detection methods for complex signals.

3.2.4 Design of complex domain anomaly metrics

In traditional anomaly detection methods, the reconstruction error is typically measured using a real-valued norm, such as calculating the difference between the predicted signal and the original signal in a real-valued space. However, for the complex signals obtained from eddy current testing, this real-valued norm only measures the difference in amplitude, ignoring phase information, and thus cannot fully reflect the feature shifts caused by anomalies. Considering that defects often

cause both amplitude attenuation and phase drift, using only a real-valued error can lead to insufficient discriminative power.

To address this, this paper proposes an amplitude-phase joint complex anomaly measure, which extends the reconstruction error from a real-valued norm to a complex-domain consistency measure. Specifically, for a true signal z and a reconstructed signal ž, we define:

$$D(z,\hat{z}) = \alpha \cdot (1 - \cos(\theta - \hat{\theta})) + (1 - \alpha) \cdot \frac{|r - \hat{r}|}{r + \hat{r} + \epsilon} (4)$$

Here, r and \hat{r} represent the amplitudes of the true and reconstructed signals, respectively; θ and $\hat{\theta}$ represent their phases; α is a weighting parameter; and ϵ is a small constant to prevent division by zero. This metric has three notable characteristics. First, it achieves an amplitude-phase joint measurement. When calculating the reconstruction error, it simultaneously considers both amplitude deviation and phase drift, preventing the omission of anomaly patterns that a single metric might miss. Second, it is robust to rotation and scaling. Since the measure is based on the relative phase difference and a normalized amplitude difference, it is insensitive to global signal rotation or scaling, which better aligns with the physical principles of eddy current signals. Third, it embodies physical consistency. Phase differences correspond to the location and nature of a defect, while amplitude differences reflect the severity of the defect. Combining the two allows for a more realistic characterization of the signal anomaly. Experimental results show that this complex anomaly measure effectively improves the stability and robustness of the detection, especially in high-noise environments, where it can still accurately distinguish between normal and abnormal signals, providing a more physically consistent optimization target for the C-TranAD model.

3.3 Training Strategies

Constructing an effective complex deep model requires not only innovative architectural design but also appropriate training strategies and numerical stability handling. C-TranAD employs a two-stage training process and includes meticulous optimizations for potential numerical issues in complex computations.

Phase 1: Complex-Domain Adversarial Training (Unsupervised Representation Learning). In the first phase, we do not use defect labels. Instead, we learn the complex feature representation of normal data through an adversarial mechanism. Specifically, we feed the time-series data X from the training set (primarily normal samples) into the model, and the encoder-decoder outputs the reconstruction \hat{X} . The training objective is, on the one hand, to minimize the reconstruction error, making \hat{X} as close as possible to the original X. On the other hand, we introduce an adversarial loss to enhance the model's sensitivity to abnormal patterns. This is achieved through a focus score mechanism: we define a focus score F in the complex domain that considers both the phase and amplitude differences between the reconstructed and true sequences. The focus score F can be understood as a geometric distance loss: it takes values in [0,1], and a larger value indicates a more significant difference between the reconstruction and the original in either phase or amplitude, suggesting a possible anomaly. We use this focus score for the model's self-regulation and adversarial training. The approach is to make the model pay more attention to the time points with

high focus scores (potential anomalies) during training, improving its reconstruction capability for these points. Simultaneously, an auxiliary discriminator (which can be seen as an internal adversarial module of the model) tries to identify the abnormal positions in the original sequence based on the focus score. Even if there are anomalies in the original sequence, the model's reconstruction should try not to reveal traces of these anomalies, making the focus score difficult to distinguish. This adversarial training style encourages the model to learn a more robust representation, preventing it from ignoring anomalies due to local minima in the reconstruction error. In short, the first training phase equips C-TranAD with the ability to reconstruct normal patterns in the complex domain. Through the focus score mechanism, it extends adversarial training to the complex geometric space, teaching the model to simultaneously consider both amplitude and phase consistency, thus more keenly capturing abnormal signals.

Phase 2: Classifier Training (Supervised Discriminative Fine-tuning). After sufficient unsupervised training, the encoder and decoder of C-TranAD have learned to effectively model normal eddy current signals. We then proceed to the second training phase: using labeled data to train the classification head to output a clear defect detection result. In this phase, we freeze or partially freeze the parameters of the main model and only optimize the parameters related to the classification head (including the branches in the aforementioned multi-scale fusion module and the final classifier). The training data consists of time-series segments with defect labels, where we assign a binary label to each input sequence (0=normal, 1=abnormal). The classification head, based on the feature representation learned in the first phase, outputs a predicted label after multiscale extraction and fusion. We use cross-entropy loss to train it. It is worth noting that since the input features to the classification head come from the already-trained complex encoder/decoder network, they naturally contain comprehensive information about phase and amplitude, as well as a memory of the normal pattern. Therefore, even with a small number of labels, the classification training can converge quickly and further enhance the model's sensitivity to anomalies, achieving end-to-end defect detection. The two-stage training strategy combines the advantages of unsupervised representation learning and supervised fine-tuning: the first stage provides a reliable feature extraction foundation, while the second stage optimizes for the specific detection task, greatly improving the final discriminative performance.

4. Experimental results and comparison

4.1 Experimental setup

We conducted evaluations using our self-built multi-frequency, multi-channel eddy current testing dataset from nuclear power plant steam generator tubes (SGT-ECT-13C5F). The data was collected during ECT inspections of steam generator tubes during a shutdown and maintenance period. It is recorded as complex impedance time-series (real/imaginary parts) with corresponding defect annotations. The dataset includes both actual in-service damage and simulated defects introduced through manufacturing processes. The signals cover multiple frequencies and channels. Normal regions present as smooth, closed-loop trajectories on the complex plane, while passing through a defect results in sudden amplitude changes or phase jumps. To ensure sample consistency, the long raw sequences were normalized and lightly denoised, then segmented into fixed-length sub-sequences using a sliding window with moderate overlap. The window

boundaries were aligned with file/label boundaries to avoid context mixing. The training set consists solely of defect-free windows to learn the normal pattern, while the test set contains both defect windows and their labels for evaluation.

The compared methods are consistent with the figures and tables, covering the traditional rule-based method Rule-ECT, the unsupervised machine learning method One-Class SVM, the complex-domain deep learning models CV-FCNN and CV-CNN, the original TranAD model in the real domain (TranAD-Real), and the proposed C-TranAD (complex domain). Except for the explicitly labeled supervised baselines, all methods were trained in an unsupervised manner, with the anomaly score threshold selected on a validation set. For models that directly output a defect probability, a fixed threshold was used for binarization. The experiments were conducted on a single machine with dual NVIDIA RTX 4090 GPUs (24 GB × 2), unified under PyTorch+CUDA for acceleration. The AdamW optimizer was used, along with a simple step-wise learning rate decay and early stopping strategy. The window length was fixed (e.g., 10), and the batch size was matched to the model complexity (larger for Transformer series, moderate for CNN/RNN models). Other training details were kept consistent to ensure fair comparison.

For evaluation, we uniformly used four metrics: Precision, Recall, F1-Score, and AUC, with abnormal samples treated as the positive class. All results were reported as mean \pm standard deviation over multiple random seeds. The setup described above, along with the subsequent tables and visualizations, is strictly followed without introducing any additional post-processing or threshold tuning.

4.2 Experimental Result Analysis

4.2.1 Comparative Analysis

The C-TranAD model is trained on a proprietary multi-frequency eddy current defect detection dataset, SGT-ECT-13C5F, using 5-fold cross-validation. The training process involves end-to-end complex-domain modeling, which preserves the amplitude-phase coupled features of the eddy current signals, and incorporates learnable complex activation functions and a hierarchical classification mechanism. As shown in Figure 7, to evaluate the model's performance in multivariable time-series anomaly detection, a range of metrics were computed, including classification boundaries, data distribution, ROC curves, classification score distributions, F1 score analysis, performance metric summaries, confusion matrices, and feature importance.

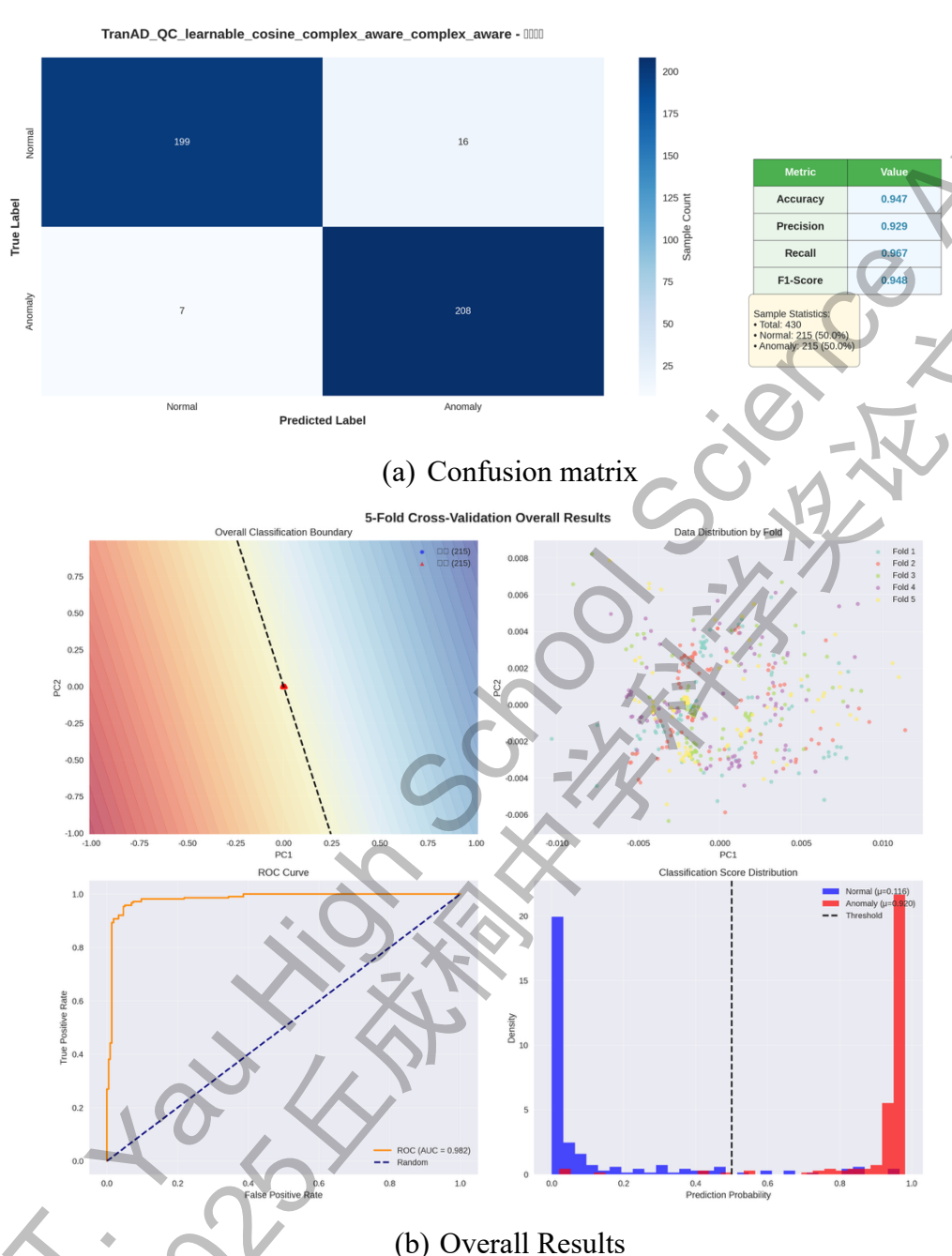


Figure 7. Performance of the model

To validate the performance of our model, we conducted a comparative experiment between the proposed C-TranAD and several baseline methods. These baselines include the traditional method Rule-ECT based on manual rules, the unsupervised machine learning method One-Class SVM, the complex-domain deep learning models CV-FCNN and CV-CNN, the original TranAD model in the real domain (TranAD-Real), and our proposed complex-domain model C-TranAD. Table 1 summarizes the average performance metrics of each model on the simulated dataset.

Table 1 The comparison results of the compared approaches on our dataset

Method	Precision(%)	Recall(%)	F1(%)	AUC(%)
Rule-ECT(rules, inuse)	84.56±5.23	85.24 _{±2.35}	84.90 _{±3.83}	N/A
One-Class SVM	79.23 _{±2.64}	81.35 _{±3.24}	80.28 _{±2.79}	84.02 _{±2.18}
CV-FCNN	89.73 _{±3.62}	85.76 _{±2.41}	87.70 _{±2.96}	88.51 _{±2.72}
CV-CNN	91.65 _{±2.83}	87.44 _{±2.33}	89.50 _{±2.37}	90.92±2.16
TranAD-Real	96.11±2.21	72.56±4.24	82.69 _{±3.20}	84.58±3.69
C-TranAD(ours)	92.86±1.26	96.74 _{±2.21}	94.76±1.65	94.65 _{±1.97}

As seen in Table 1, the performance of traditional and real-domain models is significantly lower than that of complex-domain deep learning models. C-TranAD demonstrates the best overall performance across all metrics, highlighting the superiority of the proposed method. Particularly in terms of the balance between Precision and Recall, C-TranAD achieves an F1-Score of 94.76%, which is about 5 percentage points higher than the next best, CV-CNN. At the same time, its recall rate reaches 96.74%, significantly outperforming other methods.

This indicates that C-TranAD can detect almost all defects (extremely low missed detection rate) while maintaining a very low false alarm rate. In contrast, although TranAD-Real has the highest precision (Precision=96.11%), its recall rate is only 72.56%. This suggests that the original TranAD architecture suffers from a severe missed detection problem when using only real-valued features, failing to generalize to detect diverse defect patterns.

Furthermore, traditional methods like One-Class SVM perform the worst on all metrics (F1 approx. 80%, AUC approx. 84.02%), reflecting the limited capability of such models to capture the complex characteristics of eddy current signals, resulting in high rates of both missed and false detections. In comparison, complex-domain deep neural networks like CV-FCNN and CV-CNN, by incorporating both amplitude and phase information, achieve better performance than real-domain models (F1 scores of 87.70% and 89.50%, respectively). It is noteworthy that the performance of CV-CNN is already close to that of TranAD-Real, indicating that using convolutional models on complex signals can, to some extent, compensate for the deficiencies of the Transformer architecture. However, C-TranAD builds upon this and further significantly improves both precision and recall, demonstrating that combining the Transformer architecture with full complex-domain modeling can more thoroughly exploit signal features, thus achieving optimal defect detection performance.

In conclusion, C-TranAD exhibits excellent generalization ability and robustness. Whether it is the stable detection of various types of defects or the small performance variance across different experimental runs, it demonstrates significant advantages over other methods.

4.2.2 Ablation Study Analysis

We designed an ablation study around the key components of C-TranAD to evaluate the impact of each module—the activation function, classification head, and distance metric—on the model's performance. Specifically, we tested the following four model variants: C-TranAD-SepLReLU, C-TranAD-Cardioid, C-TranAD-MLP, and C-TranAD-MSE. The results for Precision, Recall, F1, and AUC are summarized in Table 2.

Method	Precision(%)	Recall(%)	F1(%)	AUC(%)
C-TranAD- SepLReLU	92.78 _{±1.69}	77.67 _{±3.94}	84.56 _{±2.25}	85.81 _{±1.22}
C-TranAD- Cardioid	91.65 _{±2.26}	81.86±1.58	87.34±2.11	88.14±2.65
C-TranAD-MLP	93.65 _{±2.11}	82.32 _{±1.24}	87.62 _{±1.38}	88.37 _{±3.22}
C-TranAD-MSE	92.36±0.88	85.11±5.66	89.05±3.21	89.53±2.86
C-TranAD(ours)	92.86±1.26	96.74±2.21	94.76±1.65	94.65±1.97

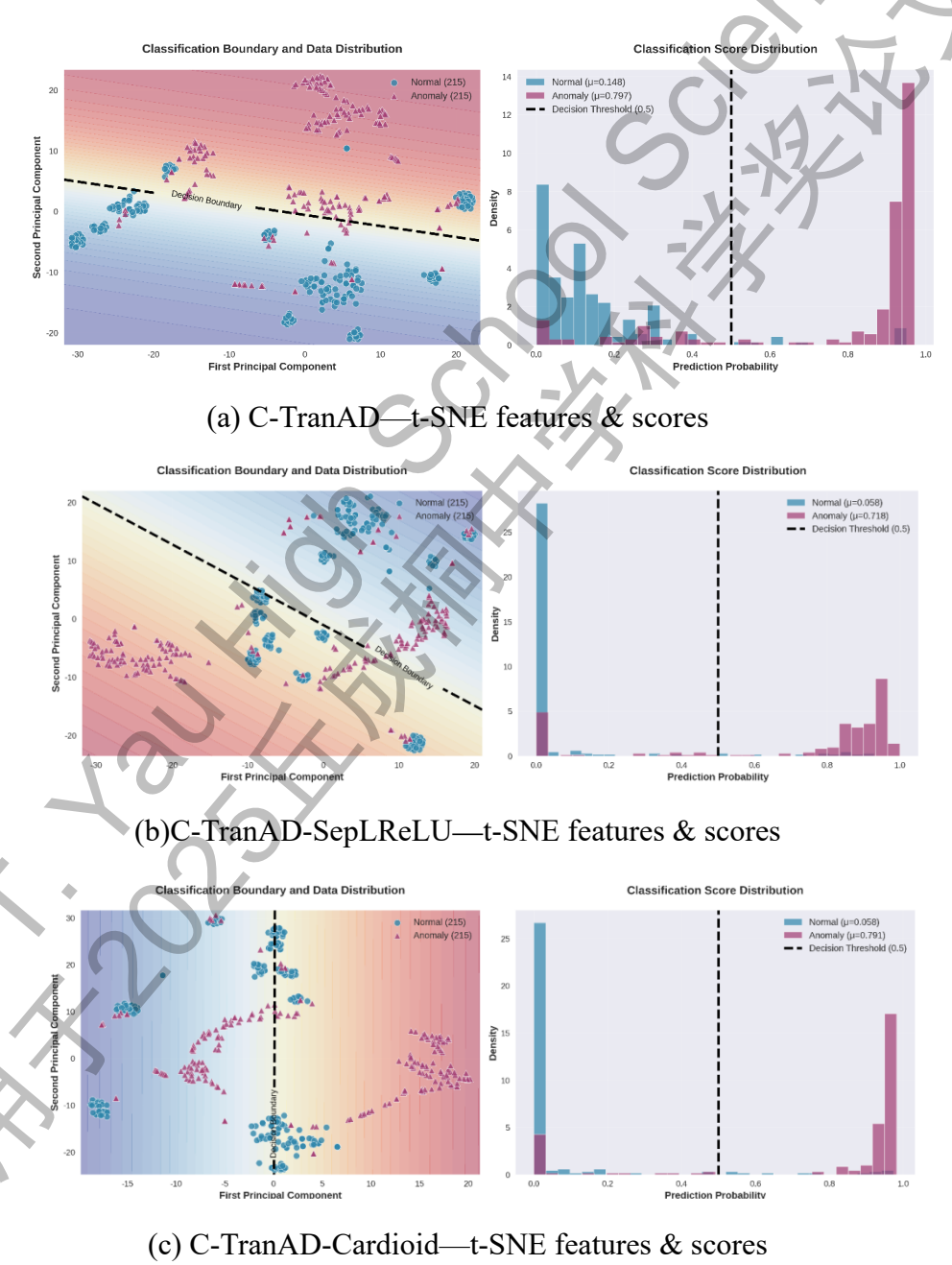
Table2 The results of Ablation Experiments on C-TranAD Components

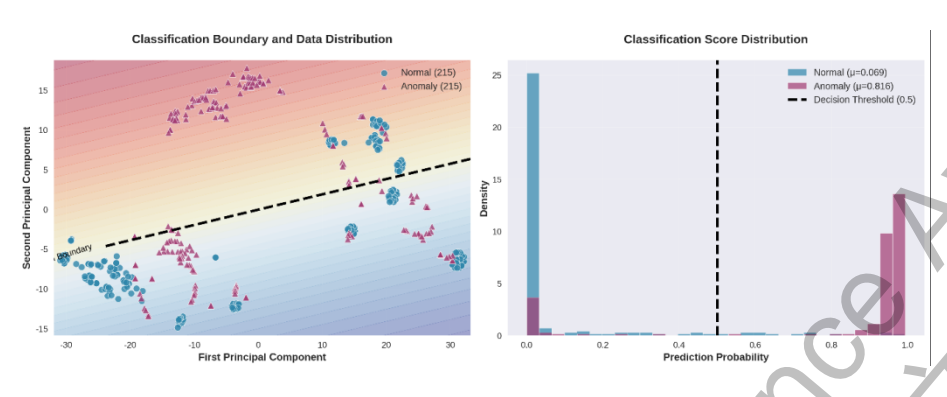
The results from the ablation study in Table 2 show that removing any of the modifications leads to a performance drop to varying degrees, indicating that each component's design plays a key role in enhancing the model's final performance. Specifically, the C-TranAD-SepLReLU variant, which uses separate activation functions for the real and imaginary parts, fails to capture the coupling between them, causing the model's recall to plummet to 77.67% and the F1 score to only 84.56%. This demonstrates that removing the complex-domain Cardioid activation function severely weakens the model's ability to detect subtle phase anomalies. The C-TranAD-Cardioid variant, which uses a fixed-parameter Cardioid activation, shows a slight improvement over SepLReLU, but due to the lack of adaptive parameter tuning, its F1 score is still about 7 percentage points lower than the original model. Replacing the classification head with a single-branch MLP in the C-TranAD-MLP variant also results in a significant performance drop (F1 drops to 87.62%) due to the lack of hierarchical discriminative capability for amplitude and phase information. Finally, the C-TranAD-MSE variant, which uses the traditional MSE distance as the anomaly criterion, achieves an F1 of 89.05%, but this is still about 5 percentage points lower than the original model, indicating that the complex-domain anomaly metric designed in this paper is effective in improving detection accuracy and robustness.

As shown in Figure 8, the original C-TranAD (Fig 8(a)) clearly separates normal and abnormal samples in the feature space, with the decision boundary almost perfectly dividing the two classes. Correspondingly, in the score distribution histogram, the score ranges for normal and abnormal samples have almost no overlap (mean score for normal samples is approx. 0.148, while for

abnormal samples it is 0.797), indicating that the model has extremely high confidence in its defect detection results, with almost no missed or false detections.

In contrast, C-TranAD-SepLReLU (Fig 8(b)), which uses separate real/imaginary activation functions, shows some overlap between normal and abnormal samples in the t-SNE space. Some abnormal points are mixed in with the normal sample cluster, forcing the model's decision boundary to compromise between the two classes, leading to an increase in missed detections. This is also reflected in the score distribution: the predicted scores for abnormal samples are not sufficiently concentrated (mean is only 0.718), with some abnormal samples having scores that fall into the range of normal samples, ultimately causing a significant drop in recall.





(d)C-TranAD-MSE— t-SNE features & scores

Figure 8. t-SNE feature space and score distributions on the EC dataset

For C-TranAD-Cardioid (Fig 8(c)) using a fixed Cardioid activation, the problem of abnormal samples being too close to normal ones is also observed. However, compared to SepLReLU, the Cardioid activation retains some phase sensitivity, so the separation between the abnormal and normal clusters is slightly better, although a few abnormal samples (purple triangles) are still near the decision boundary. The fixed activation function cannot adaptively adjust based on data features, leading to insufficient discriminative ability for samples near the boundary, which ultimately results in a certain degree of performance loss.

For the final variant, C-TranAD-MSE (Fig 8(d)), the visualization shows that the normal and abnormal samples are generally well-separated, with most abnormal points correctly classified outside the decision boundary. However, a few abnormal samples (purple triangles) are still close to the normal sample cluster and are not identified by the model. This is consistent with its score distribution: although the average score for abnormal samples is high at 0.816, and for normal samples is only 0.069, the distribution of abnormal scores shows a certain degree of spread, indicating that the model lacks confidence in discriminating a few anomalies. Overall, the model using the MSE distance metric can provide high anomaly scores for easily detectable significant anomalies, comparable to the original model, but it is less sensitive to subtle anomalies near the boundary, leading to a lower recall rate compared to the original model.

This visual comparison clearly shows that each of the proposed improvement modules (learnable complex activation functions, hierarchical classification head, and complex-domain anomaly measure) is indispensable for enhancing the model's discriminative ability and robustness. Only the complete C-TranAD model can form a clear and reliable separation between normal and abnormal samples in the feature space, ultimately achieving optimal defect detection performance.

5. Analysis and Discussion

The core of this work lies in fully exploiting the joint amplitude-phase features of eddy current signals and enhancing defect detection performance through complex-domain modeling. Both experimental and theoretical analyses show that the complex-domain method has the following significant advantages over traditional real-domain methods.

First, in terms of geometric modeling capability, the response of normal samples in eddy current inspection typically forms a stable, closed trajectory in the complex plane, while defects cause distortions or shifts in this trajectory. Traditional real-valued methods often project the signal onto a single amplitude or phase channel, making it difficult to preserve the complete trajectory shape. In contrast, complex networks can directly represent and identify the geometric changes of the trajectory in the two-dimensional complex plane, thus avoiding the loss of detailed information. The C-TranAD proposed in this paper further uses the phase angle as a modulating signal, making the network more sensitive to changes in the trajectory's direction. Thus, even if some defects primarily manifest as phase shifts with minor amplitude changes, the model can still amplify and identify them through phase-cosine modulation. For defects dominated by amplitude spikes, the activation function dynamically scales the output during rapid phase changes, achieving sharp detection in the amplitude channel. It is evident that the cooperative sensing mechanism of amplitude and phase gives C-TranAD excellent adaptability to various types of defects, which is difficult for real-valued models to achieve.

Second, in terms of multi-scale feature representation and interpretability, the hierarchical activation and classification fusion mechanism proposed in this paper endows the model with frequency-division and hierarchical capabilities. This design can be analogized to the manual analysis of eddy current signals: engineers typically examine both amplitude and phase curves simultaneously and make judgments based on information from different filter scales. Our multibranch structure and multi-modal fusion automatically achieve this process: the learnable complex Cardioid activation functions with different parameters act as frequency selectors, with each branch focusing on a specific spectral pattern. Residual connections and feature fusion ensure a balance between global and local information. Explicitly separating amplitude and phase features at the classification head stage makes the decision process closer to physical intuition. It is noteworthy that this mechanism also improves the model's interpretability: for example, for crack-like defects mainly characterized by phase perturbations, the model primarily relies on the high response of the phase branch for detection; for deep-hole defects causing a sharp drop in amplitude, it relies more on the amplitude branch. These phenomena fully validate the effectiveness of the complex-domain hierarchical mechanism.

Finally, from the perspective of the synergistic action of the activation function and the classification head, its significant effect can be understood on two levels: at a micro level, the learnable complex Cardioid activation function makes each neuron sensitive to phase changes, enhancing the quality of the low-level representation; at a macro level, the multi-scale classification head organizes and integrates these phase-sensitive representations, enabling the model to perform joint discrimination from different scales and modalities. The combination of these two achieves a bottom-up progressive optimization: low-level features progressively refine discriminative phase characteristics, and high-level multi-scale fusion forms a robust decision. This design philosophy enables C-TranAD to simultaneously capture local detail anomalies and global pattern shifts in complex eddy current backgrounds, and the experimental results have proven the significant advantages and universal potential of this complex-domain hierarchical activation and classification fusion.

6. Conclusion

In the research, we propose C-TranAD, a complex-domain deep anomaly detection model for eddy current non-destructive testing. Based on the existing TranAD framework, this method is the first to systematically extend it to the complex domain, achieving end-to-end modeling of amplitude-phase information and avoiding the information loss and complex manual feature extraction of traditional methods. To further enhance the model's expressive power, this paper innovatively introduces a parameter-learnable complex Cardioid activation function, endowing the network with a phase-driven adaptive non-linear mapping capability. It also designs a multi-scale complex classification head (V2), which, through parallel branches and a fusion mechanism, achieves a hierarchical characterization of amplitude and phase anomalies, constructing a novel complex-domain hierarchical activation-classification fusion mechanism.

Experiments on actual eddy current inspection data show that C-TranAD significantly outperforms the real-domain TranAD and various baseline methods in terms of detection accuracy and robustness. It maintains stable performance even in complex backgrounds and high-noise conditions. For challenging micro-defects, the model achieves near-zero missed detections while significantly reducing the false alarm rate, demonstrating outstanding engineering application value. Thanks to its lightweight design with only a few Transformer layers, C-TranAD's inference speed meets the real-time detection needs of industrial sites, effectively reducing the burden of manual review. From a theoretical perspective, C-TranAD organically combines the physical characteristics of complex signals (amplitude and phase) with deep learning architectures, providing a universal paradigm for complex-domain deep anomaly detection and a feasible path for the efficient utilization of phase information. In terms of engineering value, this method offers a practical solution for high-precision, low-false-alarm defect identification in eddy current NDT.

Future work can be extended in the following directions: First, expand the application scenarios by promoting the method to other typical complex signal anomaly detection tasks such as acoustic ultrasound, radar, and seismic exploration to verify its universality. Second, improve model efficiency by exploring more lightweight complex network structures or model compression strategies to meet the deployment requirements of resource-constrained devices. Third, deepen the theoretical research by systematically analyzing the mechanism of complex activation functions, studying the influence of parameters on the model's spectral response, and the convergence of complex adversarial training. Fourth, integrate physical priors by attempting to incorporate physical models of eddy current inspection or finite element simulation results into the network design and loss function to further enhance the model's interpretability and reliability.

In summary, the work in this paper not only achieves a breakthrough in the methodology of complex-domain end-to-end anomaly detection but also verifies its excellent performance and engineering practicality through experiments, marking a key step forward for the application of complex deep learning in non-destructive testing and the broader field of signal processing.

Reference

- [1] Wang C., Chai X., Yang B., et al. (2023). Development and Prospect of Advanced Nuclear Energy Technology. Nuclear Power Engineering, 44(5), 1-5.
- [2] Qian H., Jiang C., Pan, Y., et al. (2020). Research on Diagnosis of the Leakage Degree of Steam Generator Tube Based on Time Series Neural Network. Nuclear Power Engineering, 41(2), 160-167.
- [3] Tian W., Wang M., Zeng C., et al. (2022). Development and Application of Three-dimensional Nuclear Steam Generator Thermal-hydraulic Analysis Code STAF. Atomic Energy Science & Technology, 56(11).
- [4] Xiao C., Yang H., Zhang D., et al. (2024). Study on Thermal-hydraulic Steady-state Comprehensive Performance of Fast Reactor Sodium-water Steam Generator. Atomic Energy Science and Technology, 58(2), 328-336.
- [5] Xie S, Duan Z, Li J, et al. A novel magnetic force transmission eddy current array probe and its application for nondestructive testing of defects in pipeline structures[J]. Sensors and Actuators A: Physical, 2020, 309: 112030.
- [6] She S, Chen Y, He Y, et al. Optimal design of remote field eddy current testing probe for ferromagnetic pipeline inspection[J]. Measurement, 2021, 168: 108306.
- [7] Chen X, Li J, Wang Z. Inversion method in pulsed eddy current testing for wall thickness of ferromagnetic pipes[J]. IEEE Transactions on Instrumentation and Measurement, 2020, 69(12): 9766-9773.
- [8] Jin Z, Meng Y, Yu R, et al. Methods of controlling lift-off in conductivity invariance phenomenon for eddy current testing[J]. IEEE Access, 2020, 8: 122413-122421.
- [9] She S, Zheng X, Xiong L, et al. Thickness measurement and surface-defect detection for metal plate using pulsed eddy current testing and optimized Res2Net network[J]. IEEE Transactions on Instrumentation and Measurement, 2024, 73: 1-13.
- [10] Kong Y., Ma Q., Wang C., et al. (2025). Development and Application of Eddy Current Array Inspection Technology for Steam Generator Heat Transfer Tubes. Nuclear Safety, 24(3).
- [11] Ren J., & Yang P. (2022). Lifecycle Data Management of Nuclear Power Plant: Framework System and Development Suggestions. Strategic Study of CAE, 24(2), 152-159.
- [12] Mohamad A J, Ali K, Rifai D, et al. Eddy current testing methods and design for pipeline inspection system: a review[C]//Journal of Physics: Conference Series. IOP Publishing, 2023, 2467(1): 012030.
- [13] Han Y, Tao Y, Shao C, et al. Pulsed eddy currents in ferromagnetic pipes with cladding in nuclear power plants[J]. Energy Reports, 2022, 8: 104-111.
- [14] Xia Z, Yan J, Huang R, et al. Fast estimation of metallic pipe properties using simplified analytical solution in eddy-current testing[J]. IEEE Transactions on Instrumentation and

- Measurement, 2022, 72: 1-13.
- [15] Latif J, Shakir M Z, Edwards N, et al. Review on condition monitoring techniques for water pipelines[J]. Measurement, 2022, 193: 110895.
- [16] Chen T., Yin Y., Lü C., et al. (2024). Review of Theory and Technology of Pulsed Eddy Current Defect Detection. Journal of Electronic Measurement and Instrumentation, 38(9), 1-10.
- [17] Hao B., Fan Y., & Song Z. (2023). Deep Transfer Learning-Based Pulsed Eddy Current Thermography for Crack Defect Detection. Acta Optica Sinica, 43(4), 0415002.
- [18] Zhang Y., & Fan Y. (2024). Defect Detection of Eddy Current Thermal Imaging of Workpiece Based on Deep Learning and Domain Adaptation. Infrared Technology, 46(3), 347-353.
- [19] Lin L., Jiang J., Zhu J., et al. (2023). Detection and Recognition of Metal Fatigue Cracks by Bi-LSTM Based on Eddy Current Pulsed Thermography. Infrared Technology, 45(9), 982-989.
- [20] Zhang Y., Liu P., Chen L., et al. (2023). YOLO v5-based Intelligent Detection for Eddy Current Pulse Thermography of Subsurface Defects in Coated Steel Structures. Infrared Technology, 45(10), 1029-1037.
- [21] Tuli S, Casale G, Jennings N R. Tranad: Deep transformer networks for anomaly detection in multivariate time series data[J]. arXiv preprint arXiv:2201.07284, 2022.
- [22] Wang X., Teng Y., Shi P., et al. (2025). A hybrid islanding detection method based on the Lissajous Pattern and impedance for grid-forming energy storage inverter. Energy Storage Science and Technology, 14(3), 1299.
- [23] Chen B, Yu T. Complex-Valued CNN-Based Defect Reconstruction of Carbon Steel from Eddy Current Signals[J]. Applied Sciences, 2025, 15(12): 6599.
- [24] Yin L, Ye B, Zhang Z, et al. A novel feature extraction method of eddy current testing for defect detection based on machine learning[J]. Ndt & E International, 2019, 107: 102108.
- [25] Miao R, Shan Z, Zhou Q, et al. Real-time defect identification of narrow overlap welds and application based on convolutional neural networks[J]. Journal of Manufacturing Systems, 2022, 62: 800-810.
- [26] Gao S, Zheng Y, Li S, et al. Eddy current array for defect detection in finely grooved structure using MSTSA network[J]. Sensors, 2024, 24(18): 6078.
- [27] Zhang Q., Li X., Sun J., et al. (2022). Fast Solving Method for Analytical Model of Pulsed Eddy Current TR Probe. Computer Measurement & Control, 30(2).
- [28] Wang Y., Du W., & Wang S. (2021). Extracting glacier information from remote sensing imageries by automatic threshold method of Gaussian mixture model. National Remote Sensing Bulletin, 25(7), 1434-1444.
- [29] Li Y., Hu J., Xing Y., et al. (2024). Detection Method of Sea Surface Small Target Based on Improved Isolation Forest. Radar Science and Technology, 22(6), 628-636.
- [30] Wang X., Dong Y., Yu Q., et al. (2020). A Survey on Structured Support Vector

- Machines. Journal of Computer Engineering & Applications, 56(17).
- [31] Zou C, Yang F, Song J, et al. Channel Autoencoder for Wireless Communication: State of the Art, Challenges, and Trends[J]. IEEE Commun. Mag., 2021, 59(5): 136-142.
- [32] DiPietro R, Hager G D. Deep learning: RNNs and LSTM[M]//Handbook of medical image computing and computer assisted intervention. Academic Press, 2020: 503-519.
- [33] Han K, Xiao A, Wu E, et al. Transformer in transformer[J]. Advances in neural information processing systems, 2021, 34: 15908-15919.
- [34] Kim G, Kim M. Multivariate Time Series Anomaly Detection Using TranAD: Assessing the Effectiveness of Noise Generalization Techniques[J]. Available at SSRN 5238491.
- [35] Wang D, Ruan P, Xu D, et al. TranAD: A deep transformer model for fault diagnosis of lithium batteries[C]//2023 International Conference on Smart Electrical Grid and Renewable Energy (SEGRE). IEEE, 2023: 133-139.
- [36] Lee H, Hong M, Kang M, et al. A physics-driven complex valued neural network (CVNN) model for lithographic analysis[C]//Advances in Patterning Materials and Processes XXXVII. SPIE, 2020, 11326: 84-91.
- [37] Costanzo S, Flores A. CVNN-Based Microwave Imaging Approach[C]//2023 IEEE Conference on Antenna Measurements and Applications (CAMA). IEEE, 2023: 728-731.
- [38] Wang J., Li Y., & Zhang Q. (2025). Target Recognition Based on Optically Tunable Nonlinear Functions. Modeling and Simulation, 14, 670.
- [39] Shao J., & Su Z. (2023). Design of Diffractive Optical Elements with Continuous Phase Distribution Based on Machine Learning. Acta Optica Sinica, 43(3), 0323001.
- [40] Huang J, Zhou G, Yu Z, et al. Deep parallel MRI reconstruction based on a complex-valued loss function[J]. Nan fang yi ke da xue xue bao= Journal of Southern Medical University, 2022, 42(12): 1755-1764.
- [41] Zhang S., Yang J., Liu J., et al. (2020). Power Load Recovery Based on Multi-Scale Time-Series Modeling and Estimation. Transactions of China Electrotechnical Society, 35(13), 2736-2746.
- [42] Hua Q, Ma X, Yang X, et al. Swish-Cardioid CV-CNN: A Novel Complex-Valued Activation Framework for PolSAR Terrain Classification[J]. IEEE Geoscience and Remote Sensing Letters, 2025.

致谢

本研究的选题灵感来源于我父亲的工作经历。他曾在核电站担任检验人员,负责在机组大修期间对产生的大量涡流检测数据进行人工分析与判断。每次大修都会产生海量信号曲线,检验人员需要逐一查看并识别其中可能存在的缺陷。这项工作不仅要求极高的专注力和经验积累,还常常伴随着长时间的加班。这让我萌生了利用人工智能技术辅助数据分析,减轻检验人员工作负担并提高检测效率的想法。

在此,我要特别感谢我的指导老师阮锦龙与张帆老师,他们在研究方向、技术路线和论文写作等方面都给予了无偿的、全方位的指导与支持。他们不仅帮助我解决了研究中遇到的难题,更教会了我严谨的科研方法和独立的思考能力。本研究的所有成果均在导师的指导下由我独立完成。

此外,本研究的顺利完成也得益于优秀的开源项目。感谢 TranAD 开源项目为本研究提供了重要的参考和思路,感谢 PyTorch 库和 TranAD 方法的作者在 GitHub 上开源的代码,它们为我的模型实现提供了极大的便利。

在研究过程中,本人在导师的指导下确定选题方向、调研相关工作、制定研究方案,完成了数据获取、模型搭建与训练、结果整理与分析,以及最终研究报告的撰写工作。阮锦龙老师作为计算机方面的导师,在模型选择、算法实现和代码调试等技术方面提供了宝贵的指导意见。张帆老师则在研究报告的撰写、研究可行性分析以及方法与创新点的凝练上提供了专业的指导,尤其帮助我完善了论文的结构组织和表达逻辑。

在初期遇到的主要困难是要确定选题的可行性。我自己对于深度学习在时间序列分析领域的应用理解有限,要将其应用到复杂的工业涡流信号检测中,涉及到信号处理和时序异常检测等对我来说较为陌生的领域。为了解决这一问题,我与导师进行了多次讨论。老师建议我深入阅读与时间序列异常检测相关的文献,了解该领域现有的研究成果与技术手段。在老师的指导下,我查阅了大量基于深度学习的工业时间序列分析论文,认识到Transformer模型在捕捉序列依赖关系中的广阔应用前景。这不仅帮助我更好地理解了研究课题的前沿进展,还让我有了更多的信心去探索这一选题,并且从技术上评估其可行性。在实验阶段遇到的主要困难是模型框架代码的搭建.为了解决这个问题,我通过调研发现了TranAD等前沿方法的开源代码仓库,这对我的工作具有非常高的参考价值。通过分析这些代码的思路和实现,我成功搭建了C-TranAD的基础框架,为后续的模型调整和优化打下了重要基础。